Yang and Jiu-Sheng *Journal of the European Optical Society-Rapid Publications* (2017) 13:12
DOI 10.1186/s41476-017-0039-7

Journal of the European Optical Society-Rapid Publications

RESEARCH Open Access

Numerical analysis of temperature-controlled terahertz power splitter

Li Yang and Li Jiu-Sheng*

Abstract

Background: As a significant terahertz functional device, terahertz beam splitters with high performance are highly required to meet the need for terahertz communication, terahertz image, and terahertz sensor systems.

Results: The proposed 1×6 power splitter becomes 1×4 power splitter with the aid of the localized temperature change at the frequency of 1.0THz. The total output power is equivalent to 97.8% of the input power for the six-channel splitter and 95.4% for the four-channel splitter. The dimension of the device is of 35*a*×27*a*.

Conclusions: A temperature-controlled terahertz power divider based on photonic crystal multimode interference structure and Y-junction photonic crystal waveguides is an efficient mechanism for the power divider of terahertz waves. The proposed device paves a promising way for the realization of terahertz wave integrated device.

Keywords: Terahertz wave, Tunable power splitter, Photonic crystal

Background

With the rapid development of terahertz technology, it becomes very critical and urgent to control the terahertz wave transmission efficiently. Nowadays, to manipulate the terahertz wave propagation has been one of the intensively hot research topics in both science and engineering fields. The devices for manipulation the terahertz wave include such as filters, power dividers, switches, de-multiplexers, absorbers, modulators, and so forth [1–5]. Power splitter is one key component in terahertz wave communication system, therefore, it becomes particularly important to study a terahertz power divider with high performance. In recent years, there have some research reports on the power divider in the literatures [6–12]. For example, in [8], C. Berry et. al. proposed a terahertz beam splitter using sub-wavelength silver grating fabricated on a high-density polymer substrate. In [9], C. Homes et. al. employed a thick silicon wafer as beam splitter for far-infrared and terahertz spectroscopy. In [10], B. Ung et. al. fabricated a terahertz beam-splitter based on low-density polyethylene plastic sheeting coated with a conducting silver layer. In [11] J.Li et. al. designed a terahertz wave polarization beam splitter using a cascaded multimode interference structure. In [12] T. Niu et. al. demonstrated a terahertz beam splitter based on periodic sub-array. For current beam splitters, there still exist some problems, such as large dimensions, the need for multilayer structures, and with non-tunable, etc. As a significant terahertz functional device, terahertz beam splitters with high performance are highly required to meet the need for terahertz communication, terahertz image, and terahertz sensor systems.

In this work, we propose a temperature-controlled multi-channel terahertz wave power splitter based on Y-junction photonic crystal waveguides and multi-mode interference photonic crystal structure (see Fig. 1). Using the localized high-temperature in photonic crystal, we can shift the frequency position of the guide mode in photonic crystal waveguide and efficiently manipulate the output port power of the device. Both the plane wave expansion method and the finite-difference time-domain method are performed to investigate the mode properties and the transmission characteristics of the temperature-controlled terahertz power splitter. Interestingly, our results may pave the way for designing a tunable multi-channel terahertz power splitter using localized temperature-controlled photonic crystal for the thermo-optic effect. Using such a terahertz beam splitter, the whole length of the device is reduced to about 1/10 that of a conventional design [11].

* Correspondence: lijsh2008@126.com
Centre for THz Research, China Jiliang University, Hangzhou 310018, China

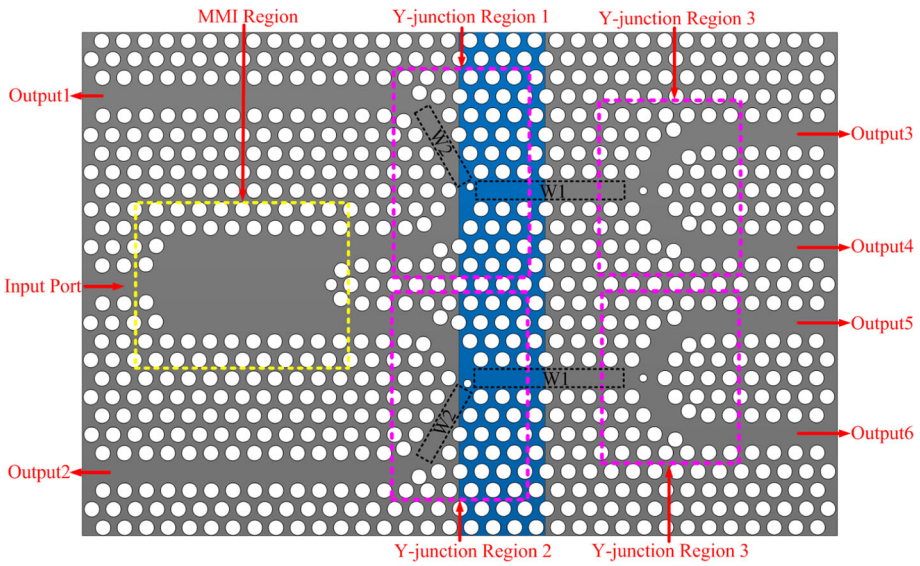

Fig. 1 Configuration of the proposed tunable multi-channel terahertz wave power splitter

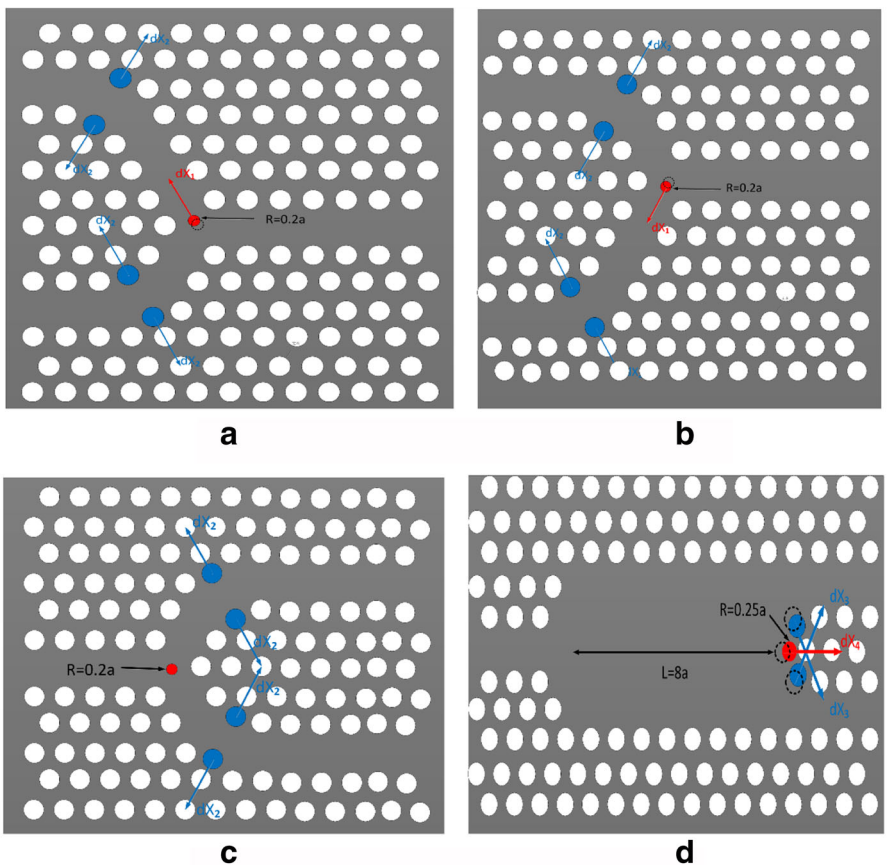

Fig. 2 Configuration of Y-junction and MMI region, **a** Y-junction Region 1, **b**Y-junction Region 2, **c** Y-junction Region 3, **d** MMI Region

Device design

The schematic view of the proposed temperature-controlled multi-channel terahertz power splitter is shown in Fig. 1. In this figure, the device consists of four photonic crystals Y-junction waveguides (marked with Y-junction Region 1, Y-junction Region 2, and two Y-junction Region 3), and a multi-mode interference structure (marked with MMI Region). A two-dimensional photonic crystal consists of a triangular lattice array of air holes with the radius of $r = 0.32a$. The localized high-temperature area in the photonic crystal is marked by using light blue. The background material is high resistivity silicon with refractive index of 3.45 (a is lattice constant of the structure). Here, the loss of the silicon with high resistivity is very weak. In the Y-junction Region 1 and 2, there have two photonic crystal waveguides named with W1 and W2. Both W1 and W2 regions are surrounded by dotted lines. Figure 2 shows the details of the three kinds of photonic crystal Y-junctions region and a MMI region. The photonic crystal Y-junction region has two 60° waveguide bends. In this study, we adjust two air hole's position shown in light blue air holes (see Fig. 2a, b and c). The air holes with the radius of $r = 0.32a$ are moved oppositely along the symmetric axis of the bend with $dx_2 = 0.26a$ [13]. Furthermore, to overcome the mode-mismatch of the Y-junction, in the middle of the Y-junction region, another air hole is introduced (marked with red), and the radius of the air hole is $r = 0.2a$. In additional, in Fig. 2a and b, the red air hole are moved along the arrows with $dx_1 = 0.3a$. To reduce the reflection of the MMI region, we optimize the MMI region by adjusting some air holes as shown in Fig. 2d. The radius of the red air hole with $r = 0.25a$ is moved along the red arrow with $dx_4 = 0.3a$. Similarly, the blue air holes are moved along the blue arrows with $dx_3 = 0.2a$. In our design, very importantly, small changes of the guide mode cut-off frequency can cause dramatic change the terahertz output intensity by the partially controlled temperature photonic crystal with thermo-optic effect. The value of the thermo-optic coefficient of silicon photonic crystal estimated from a variety of different studies reported in the literature averaged approximately $2.4 \times 10^{-4}℃^{-1}$ [14–19]. Then, the refractive index change of the temperature-controlled photonic crystal material is calculated by $\Delta n = (n - n_0) = \Delta T \times 2.4 \times 10^{-4}℃^{-1}$. At room temperature ($T = 25$ °C), the refractive index of the photonic crystal material is $n_0 = 3.45$. In this letter, to realize the function of temperature-controlled terahertz power splitter, the refractive index change of the photonic crystal is set to be 0.15 (At this time, $T = 650$ °C.) in the blue photonic crystal region as shown in Fig. 1.

According to the self-imaging principle in MMI waveguides, a self-image will be reproduced at the position of L, which can be calculated by [20]

$$L = m(3L_\pi) \tag{1}$$

where m denotes the periodic number of imaging along the multi-mode photonic crystal waveguide ($m = 0, 1, 2, \ldots$), L_π is defined as the beat length of the two lowest-order modes which is the position of the two-fold image first emerges and can be expressed by

$$L_\pi = \pi(\beta_0 - \beta_1) \tag{2}$$

where β_0 and β_1 are the propagation constants of the fundamental and the lowest-order even modes, respectively. In the MMI region, the exciting field entering the multimode waveguide is symmetric. Therefore, in our design, only even modes will be excited. To demonstrate the validity of our proposed method, the theoretically calculated L has been checked by numerical simulation according to the two-fold image mechanism.

Figure 3 shows the dispersion curves of MMI region in our presented devices by use of the plane-wave expansion method at room temperature of 25 °C. It can be noted that five guide modes (marked with 0^{th}, 1^{st}, 2^{nd}, 3^{rd} and 4^{th}) can propagate in the MMI region. Note that there is an absolute photonic band-gap within the normalized frequency range from 0.213 (a/λ) to 0.294 (a/λ) (see the blue solid lines). Here, a is lattice constant, λ is the wavelength in free space. According to Eq. (2) and Fig. 3, β_0 and β_1 refer to the 0^{th} and 2^{nd} mode, respectively. Thus, we can obtain the $\beta_0 = 0.48 \times 2\pi/a$ and $\beta_1 =$

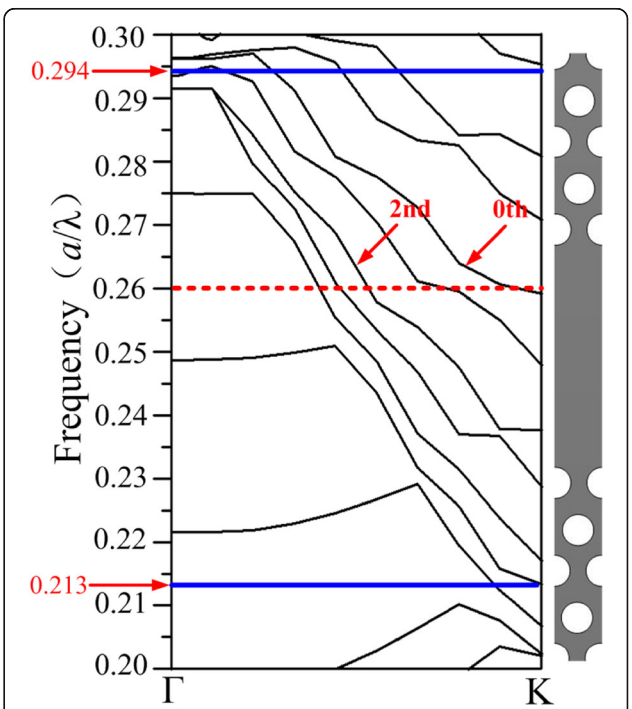

Fig. 3 Dispersion curves for the MMI region and the insert computational super cell

$0.27 \times 2\pi/a$. Substituting $\beta_0 = 0.48 \times 2\pi/a$ and $\beta_1 = 0.27 \times 2\pi/a$ into the Eq. (1) with $m = 1$ (The length of MMI region is set to be the same length of the first self-image), and then we can get $L = 3L_\pi = 7.14a$. One can see that multiple guided modes exist for almost all the frequencies in the complete photonic band gap, and all of them may operate in the photonic crystal waveguide. Therefore, in this letter, the working frequency point is set to be 0.26 (a/λ) (i.e. $f = 1$THz), and the lattice constant is $a = 78$ μm.

Figure 4 depicts the dispersive relation of the W1 and W2 waveguides for the TM-polarization. The region between the two blue solid lines indicates the complete photonic band-gap, which is for the frequency range of 0.213 $(a/\lambda) \sim 0.294$ (a/λ). According to Fig. 4a, for W1 waveguide, one sees that there have a photonic band-gap in the frequency region from 0.263 (a/λ) to 0.267 (a/λ) for TM-polarization mode (see the red shaded region in the Fig. 4a) at 25 °C. When the localized photonic crystal temperature becomes 650 °C, the photonic band-gap in the ranges from 0.253 (a/λ) to 0.256 (a/λ) for TM-polarization mode (see the green shaded region in the Fig. 4a). Since the working frequency range is set to be 0.26 (a/λ) as mentioned above (see the red dash line in the Fig. 4a), the guide mode can propagate in W1 waveguide at the localized photonic crystal temperature with 25 °C and 650 °C. From Fig. 4b, for W2 waveguide, it can be observed that there have a photonic band-gap in the region of 0.263 $(a/\lambda) \sim 0.267$ (a/λ) for TM polarization mode at 25 °C. Similarly, when the localized photonic crystal temperature becomes 650 °C, a photonic band-gap changes the frequency region of 0.258 $(a/\lambda) \sim 0.262$ (a/λ) for TM-polarization mode (see the green shaded region in the Fig. 4b). In this case, for the working frequency of 0.26 (a/λ) (see the red dash line in the Fig. 4b), the TM polarization mode can propagate through photonic crystal waveguide W2 at the localized temperature of 25 °C while it can not pass through W2 at the localized photonic crystal temperature of 650 °C. Note that the terahertz wave in the presented terahertz beam splitter is controlled by changing of the localized photonic crystal temperature.

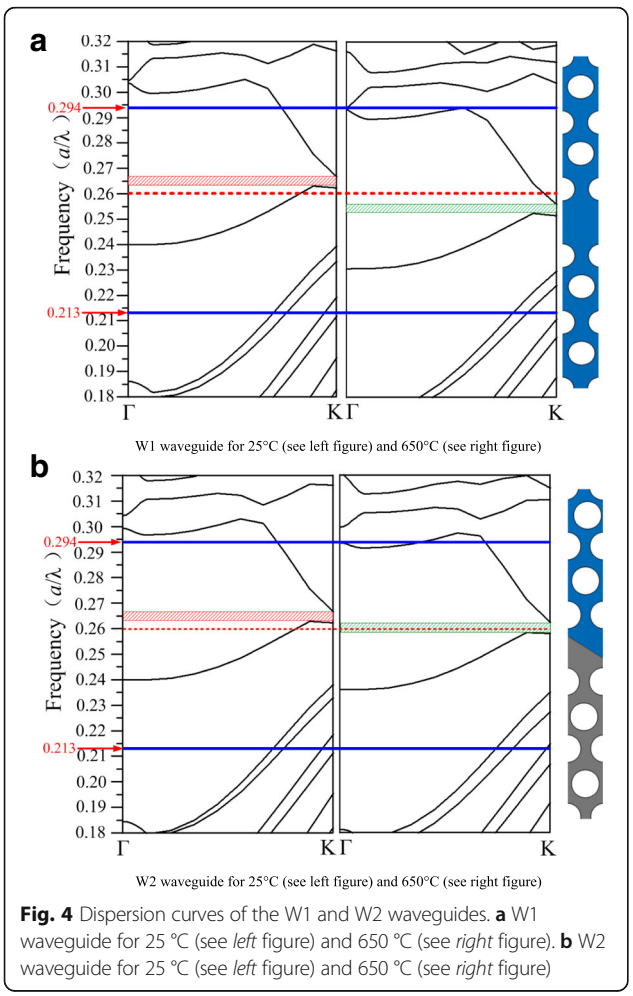

Fig. 4 Dispersion curves of the W1 and W2 waveguides. **a** W1 waveguide for 25 °C (see *left* figure) and 650 °C (see *right* figure). **b** W2 waveguide for 25 °C (see *left* figure) and 650 °C (see *right* figure)

Methods

In order to be more intuitive understanding, a commercial available software module Rsoft FullWave with the finite-difference time-domain method, is employed to simulate the terahertz wave propagation in the proposed device (see Fig. 1). The perfectly matched layers are located around the designed structure as the absorbing boundary condition. The fineness of the finite-difference time-domain cells (i.e. Δx and Δy) are set as 0.05. The Δt coefficient is 0.95 and the total calculation time is 50,000. In order to excite photonic crystal waveguide mode in the device, a continuous wave source is lunched at the input port of the photonic crystal waveguide.

Results and discussions

As the temperature of the blue photonic crystal region is 25 °C, Fig. 5a shows the steady state field distribution. According to the Figure, the terahertz wave transmits through the four Y-junction photonic crystal waveguides and a multi-mode interference photonic crystal structure, finally distributes its energy into six output ports with the equal power. In Fig. 5b, the input terahertz wave is equally distributed in the four output ports, i.e., from output 3 to output 6, when the temperature of the blue photonic crystal region becomes 650 °C. In order to investigate the structure quantitatively, we have also calculated the output power as a function of the working frequency, as shown in Fig. 6. In Fig. 6a, for the six-channel power splitter, the output power of each output port can reach a maximum of 16.5% at 1.0THz, and its corresponding total output power is of 97.8%. At this time,

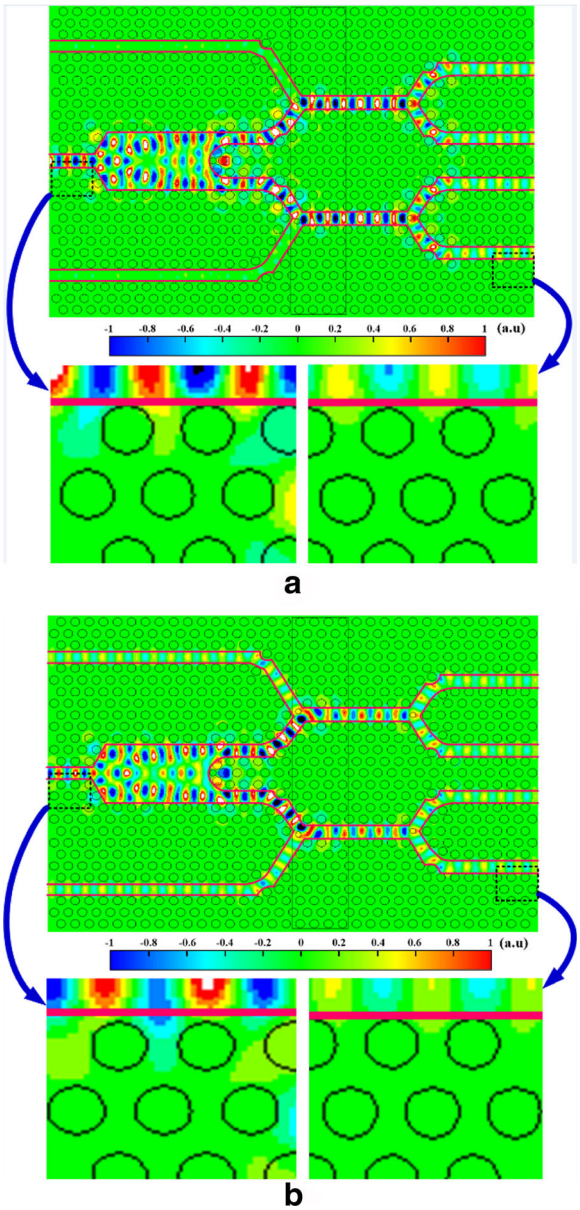

Fig. 5 Steady state electric field distribution in the proposed terahertz wave power splitter (with $f = 1$THz) at **a** 25 °C, **b** 650 °C

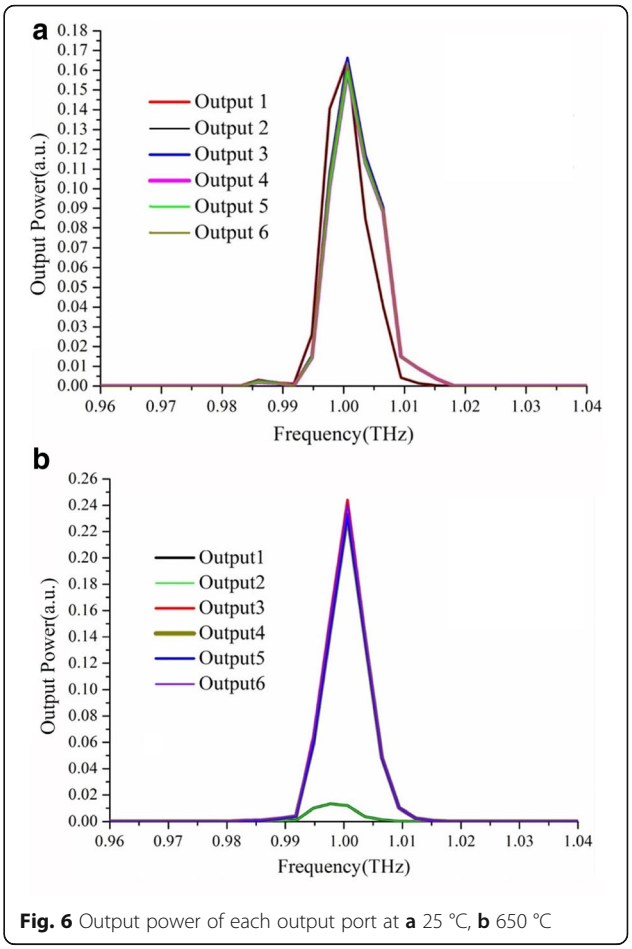

Fig. 6 Output power of each output port at **a** 25 °C, **b** 650 °C

the localized photonic crystal temperature is 25 °C. For the four-channel power splitter, the output power of each output port can reach a maximum of 24.4% at 1.0THz, and its corresponding total output power is of 95.4%, indicated by Fig. 6b. At this time, the localized photonic crystal temperature is 650 °C. The detail output powers of each output port are collected in Table 1. The simulated propagation pattern of electric field agrees well with the theoretical calculated prediction results. The total size of the whole device is of $35a \times 27a$ (i.e. 2.73×2.11 mm^2), which is about 1/10 that of a conventional design [11]. The waveguiding loss could be significantly reduced by using crystalline or polymer material featuring low absorption in terahertz region. For instance, the proposed terahertz power splitter could be manufacture from sapphire or high-resistivity silicon using the advanced methods of shaped crystal growth, such as edge-defined film-fed growth (EFG) technique (or Stepanov technique) [21]. Moreover, it could be made of polymers (such as COC, HDPE, or TPX) by implementing drawing [22] or additive manufacturing (2D and 3D printing) principles [23]. Obviously, the geometry of proposed structure should be adjusted for the refractive index of the particular material, and for its temperature-induced changes.

Table 1 Output power of each output port

Temperature	Output power					
	Output 1	Output 2	Output 3	Output 4	Output 5	Output 6
25 °C	16.5%	16.5%	16.5%	15.9%	15.9%	16.5%
650 °C	1.3%	1.3%	23.3%	24.4%	23.3%	24.4%

Conclusions

To sum up, we have designed a temperature-controlled power splitter based on photonic crystal operating in the terahertz regime. The terahertz wave power splitter was evaluated using plane wave expansion and finite-difference time-domain method. The calculated and simulated results shows that the proposed power splitter constituted by four Y-junctions and a multi-mode interference structure with embedded localized temperature-controlled photonic crystal, which can be tuned by changing the external applied temperature. The numerical simulation results are quite consistent with the analytical predictions. The design proposed here is more amenable to fabrication and also offers greater flexibility in applications of terahertz manipulation devices.

Acknowledgments

The authors would like to thank anonymous reviewers for their valuable comments to make the paper suitable for publication.

Funding

This work was supported by the National Natural Science Foundation of China Grant No. 61379024.

Authors' contributions

YL designed and performed simulations, and analyzed data. JL performed simulations, prepared the finally drafted the manuscript and the revised manuscript. Both authors read and approved the final manuscript.

Competing interests

The authors declare that they have no competing interest.

Publisher's Note

Received: 15 November 2016 Accepted: 31 March 2017
Published online: 12 April 2017

References

1. Lee, S., Choi, M., Kim, T., Lee, S., Liu, M., Yin, X., Choi, H., Lee, S., Choi, C., Choi, S., Zhang, X., Min, B.: Switching terahertz waves with gate-controlled active graphene metamaterials. Nat. Mater. **9**, 3433–3439 (2012)
2. Zhang, H., Guo, P., Chen, P., Chang, S.: Liquid-crystal-filled photonic crystal for terahertz switch and filter. J. Opt. Soc. Am. B **26**, 101–107 (2009)
3. Tao, H., Bingham, C., Strikwerda, A., Pilon, D., Shrekenhamer, D., Landy, N., Fan, K., Zhang, X., Padilla, W., Averitt, R.: Highly flexible wide angle of incidence terahertz metamaterial absorber: Design, fabrication, and characterization. Phys. Rev. B. **78**, 241103(R) (2008)
4. Robinson, S., Nakkeeran, R.: Investigation on two dimensional photonic crystal resonant cavity based bandpass filter. Optik **123**, 451–457 (2012)
5. Rodriguez, B., Yan, R., Kelly, M., Fang, T., Tahy, K., Hwang, W., Jena, D., Liu, L., Xing, H.: Broadband graphene terahertz modulators enabled by intraband transitions. Nat. Commun. **3**, 780 (2012)
6. Xiao, S., Qiu, M.: Surface-mode microcavity. Appl. Phys. Lett. **87**, 111102 (2005)
7. Park, I., Lee, H., Kim, H., Moon, K., Lee, S., Hoan, B., Park, S., Lee, E.: Photonic crystal power-splitter based on directional coupling. Opt. Express **12**, 3599 (2004)
8. Berry, C., Jarrahi, M.: Broadband terahertz polarizing beam splitter on a polymer substrate. J. Infrared Millim. Terahz. Waves **33**, 127–130 (2012)
9. Homes, C., Carr, G., Lobo, R., LaVeigne, J., Tanner, D.: Silicon beam splitter for far-infrared and terahertz spectroscopy. Appl. Opt. **46**, 7884 (2007)
10. Ung, B., Fumeaux, C., Lin, H., Fischer, B., Ng, B., Abbott, D.: Low-cost ultra-thin broadband terahertz beam-splitter. Opt. Express **20**, 4968 (2012)
11. Li, J., Liu, H., Zhang, L.: Terahertz wave polarization beam splitter using a cascaded multimode interference structure. Appl. Opt. **53**, 5024 (2014)
12. Niu, T., Withayachumnankul, W., Upadhyay, A., Gutruf, P., Abbott, D., Bhaskaran, M., Sriram, S., Fumeaux, C.: Terahertz reflectarray as a polarizing beam splitter. Opt. Express **22**, 16148 (2014)
13. Ren, G., Zheng, W., Zhang, Y., Wang, K., Du, X., Xing, M., Chen, L.: Mode analysis and design of a low-loss photonic crystal 60° waveguide bend. J. Lightwave Technol. **26**, 2215 (2008)
14. Jellison, G., Burke, H.: The temperature dependence of the refractive index of silicon at elevated temperatures at several laser wavelengths. J. Appl. Phys. **60**, 841–843 (1986)
15. Corte, F., Montefusco, M., Moretti, L., Rendina, I., Cocorullo, G.: Temperature dependence analysis of the thermo-optic effect in silicon by single and double oscillator models. J. Appl. Phys. **88**, 7115–7119 (2000)
16. Cocorullo, G., Corte, F., Rendina, I.: Temperature dependence of the thermo-optic coefficient in crystalline silicon between room temperature and 550 K at the wavelength of 1523 nm. Appl. Phys. Lett. **74**, 3338 (1999)
17. Ghosh, G.: Temperature dispersion of refractive indices in crystalline and amorphous silicon. Appl. Phys. Lett. **66**, 3570 (1995)
18. Tinker, M., Lee, J.: Thermal and optical simulation of a photonic crystal light modulator based on the thermo-optic shift of the cut-off frequency. Opt. Express **13**, 7176–7188 (2005)
19. Tinker, M., Lee, J.: Thermo-optic photonic crystal light modulator. Appl. Phys. Lett. **86**, 221111 (2005)
20. Soldano, L., Pennings, E.: Optical multi-mode interference devices based on self-imaging principles and applications. J. Lightwave Technol. **13**, 615–627 (1995)
21. Zaytsev, K., Katyba, G., Kurlov, V., et al.: Terahertz photonic crystal waveguides based on sapphire shaped crystals. IEEE Trans. Terahertz Sci. Technol. **6**(4), 576–582 (2016)
22. Nielsen, K., Rasmussen, H., Adam, A., et al.: Bendable, low-loss topas fibers for the terahertz frequency range. Opt. Express **17**(10), 8592 (2009)
23. Ma, T., Guerboukha, H., Girard, M., et al.: 3D printed hollow-core terahertz optical waveguides with Hyper uniform disordered dielectric reflectors. Adv. Opt. Mater. **4**(12), 2085–2094 (2016)